Dyes and Pigments 84 (2010) 229–236

Contents lists available at ScienceDirect

Dyes and Pigments

journal homepage: www.elsevier.com/locate/dyepig

New second-order nonlinear optical polyphosphazenes: Convenient postfunctionalization synthetic approach and application of the concept of suitable isolation group

Qi Zeng [a], Guofu Qiu [b], Cheng Ye [c], Jingui Qin [a], Zhen Li [a,*]

[a] Department of Chemistry, Hubei Key Lab on Organic and Polymeric Opto-Electronic Materials, Wuhan University, Wuhan 430072, China
[b] College of Pharmacy, Wuhan University, Wuhan 430072, China
[c] Organic Solids Laboratories, Institute of Chemistry, The Chinese Academy of Sciences, Beijing 100080, China

ARTICLE INFO

Article history:
Received 24 June 2009
Received in revised form
11 September 2009
Accepted 14 September 2009
Available online 1 October 2009

Keywords:
Polyphosphazene
Nonlinear optics
Postfunctionalization
Azo coupling
Suitable isolation groups
Structural modification

ABSTRACT

The concept of *suitable isolation group* was applied to the synthesis of nonlinear optical polyphosphazenes that contained different isolation groups attached to the side chains of polyphosphazenes using a post-functional strategy. The loading density of NLO chromophore moieties in the polymers was relatively high (0.60 per unit) and all polymers displayed good processability and relatively good NLO effects, as exemplified by an SHG coefficient (d_{33}) of 67.3 pm V^{-1} recorded for the polyphosphazene that contained the largest isolation group.

1. Introduction

Polyphosphazenes possess a unique inorganic backbone based on a repeating unit of alternating phosphorus and nitrogen atoms, bearing two substituent units on each phosphorous. Since Allcock et al. [1] synthesised the first soluble and stable polyphosphazene in 1965, literally, hundreds of divers examples of such compounds have been reported and their manifold applications as functional polymeric materials, such as fire-resistant polymers, biomedical materials, responsive membranes, battery electrolytes, fuel cell membranes, superhydrophobic surfaces, as well as nonlinear optical (NLO) polymers, reported [2–12].

Second-order nonlinear optical materials have attracted much attention owing to their potential application in photonics because of their characteristic large NLO coefficients, ultrafast response time and ease of integration [13–24]. In 1991, a second-order nonlinear optical (NLO) chromophore, Dispersed red-1 (DR-1), was attached to the backbone of polyphosphazene by Allcock et al. [25]. Improvement in the properties of NLO polyphosphazene, including NLO coefficient, loading density of NLO chromophore moieties and glass transition temperature (T_g), have been reported [26–32]. As a promising candidate for NLO polymeric materials, polyphosphazenes offer many advantages, such as high thermo-oxidative and photochemical stability and transparency of the backbone over the range, 200 nm to near-IR; additionally, the two reactive sites on each repeat unit enable good synthesis flexibility. However, the improvement in NLO properties achieved thus far has not been significant enough to satisfy all required NLO applications because of two reasons namely, the difficulty of preparing soluble NLO polyphosphazenes of high loading density of NLO chromophore moieties and synthesis difficulties caused by strong dipole–dipole interactions between the highly polar chromophoric moieties in the polymeric system. Recent research has demonstrated that according to the site isolation principle, the NLO effect of polymeric materials can be improved dramatically by the introduction of isolation spacers to the azo chromophores, which weaken the intermolecular dipole–dipole interactions between the chromophoric moieties [33–36]. The current authors have prepared different kinds of NLO polymers, in which the size of the isolation groups ranged from small to larger [37–49]. It was found that the macroscopic nonlinearity of polymers could be boosted greatly by introducing “suitable isolation group”. Interestingly, our recent research has

---

[*] Corresponding author. Tel.: +86 27 62254108; fax: +86 27 68756757.
E-mail address: lizhen@whu.edu.cn (Z. Li).

0143-7208/$ – see front matter © 2009 Elsevier Ltd. All rights reserved.
doi:10.1016/j.dyepig.2009.09.008

revealed that the both the solubility and processibility of the polymers can be improved after isolation groups have been introduced [47,48].

It was therefore considered that the introduction of isolation groups within the side chain of polyphosphazenes may solve the two problems mentioned above, namely, enhance macroscopic nonlinearity and improve solubility. This paper concerns the synthesis of a series of NLO polyphosphazenes (**P2–4**), that bear NLO chromophoric side chains with different isolation spacers, using a postfunctionalization strategy. The loading density of the chromophore moieties in the polymers was as high as 0.60 per unit, a level of substitution that could not easily be realised using the conventional direct approach for the preparation of functional polyphosphazenes. All polymers were soluble in polar organic solvents and demonstrated good processability. Second harmonic generation (SHG) experiments confirmed that after the introduction of isolation groups, the SHG coefficients (d_{33}) of **P2**–**P4** increased from 33.2 to 67.3 pm V^{-1}, in accordance with an increase in the size of the bound isolation group.

2. Experimental

2.1. Instrumentation

^{1}H and ^{13}C NMR spectra were measured on a Varian Mercury300 spectrometer using tetramethylsilane (TMS; $\delta = 0$ ppm) as internal standard. The Fourier transform infrared (FTIR) spectra were recorded on a PerkinElmer-2 spectrometer in the region of 3000–400 cm^{-1} on NaCl pellets. UV–visible spectra were obtained using a Schimadzu UV-2550 spectrometer. GPC analysis was performed on an Agilent 1100 series HPLC system and a G1362A refractive index detector. Polystyrene standards were used as calibration standards for GPC. THF was used as an eluent and the flow rate was 1.0 mL/min. EI-MS spectra were recorded with a Finnigan PRACE mass spectrometer. Elemental analyses were performed by a CARLOERBA-1106 micro-elemental analyzer. Thermal analysis was performed on NETZSCH STA449C thermal analyzer at a heating rate of 10 °C/min in nitrogen at a flow rate of 50 cm^3/min for thermogravimetric analysis (TGA). The thermal transitions of the polymers were investigated using a METTLER differential scanning calorimeter DSC822e under nitrogen at a scanning rate of 10 °C/min. The thermometer for measurement of the melting point was uncorrected. The thickness of the films was measured with an Ambios Technology XP-2 profilometer.

2.2. Materials

Tetrahydrofuran (THF) was dried over and distilled from K–Na alloy under an atmosphere of dry nitrogen. *N*-Methylpyrrolidone (NMP; caution: decomposes upon exposure to light; combustible; incompatible with strong oxidizing agents, strong acids, reducing agents, bases) was dried over and distilled from CaH_2 under an atmosphere of dry nitrogen. Compounds **9** were obtained as reported in our previous work [49]. All other reagents were used as received.

2.3. Synthesis of *P0*

N-Ethyl-*N*-hydroxyethylaniline (1.91 g, 11.6 mmol) reacted with sodium hydride (caution: corrosive; reacts violently with water, liberating hydrogen; incompatible with water, acids, alcohols, strong oxidizing agents) (0.46 g, 60% in paraffine, 11.6 mmol) in THF (20 mL) at 60 °C overnight, then the resultant solution of the sodium salt of compound **1** was added to a solution of poly(dichlorophosphazene) (caution: toxic; flammable; reacts violently with water; contact with water liberates flammable gases; explosive when mixed with oxidizing substances; may form explosive peroxides) (0.64 g, 5.5 mmol) in 80 mL of THF, and the mixture was stirred at 60 °C for 2 days. Then $NaOCH_2CH_3$ (0.79g, 11.6 mmol) was added, and the resultant mixture stirred at 60 °C for another 2 days. The mixture was poured into water (400 mL), and the white solid was filtered, washed with water, and air-dried. The solid was dissolved in THF, and the insoluble residue was filtered out. The filtrate was evaporated to remove the bulk of THF. Then the solid was isolated and further purified by several precipitations from THF into methanol. The solid was vacuum-dried at 40 °C to yield the product (1. 20 g, 74.0%). $M_w = 1\,460\,000$, $M_w/M_n = 2.73$ (GPC, polystyrene calibration). ^{1}H NMR ($CDCl_3$): δ (ppm): 0.3–1.1 ($-CH_3$), 2.5–3.5 ($-OCH_2-$ and $-NCH_2-$), 3.5–4.2 ($-OCH_2-$), 6.0–6.6 (ArH), 6.6–7.2 (ArH).

2.4. Synthesis of *P1*

P0 (0.70 g) was dissolved in *N*-methylpyrrolindone (NMP, 3.4 mL), and then 2-(2-hydroxyethoxy)-4-nitrobenzenediazonium fluoroborate (caution: author needs to add cautionary advice here) (0.71 mg, 2.4 mmol) was added under cooling with an ice bath. The color of the solution changed to red immediately. After stirring for 8 h at 0 °C, excess anhydrous potassium carbonate was added, and the mixture was stirred for additional 1 h and then filtered. The residue was washed with DMF, the filtrates were collected, and DMF was removed under reduced pressure. Some methanol was added dropwise to precipitate the polymer. The solid was further purified by several precipitations from DMF into methanol. The solid was dried in a vacuum at 40 °C to yield a red product **P1** (0.92 g, 89%). ^{1}H NMR (DMSO-d_6): δ (ppm): 0.4–1.1 ($-CH_3$), 3.4–3.8 ($-CH_2O$), 3.8–4.2 ($-CH_2O$, $-NCH_2-$), 6.2–6.8 (ArH), 6.8–7.0 (ArH), 7.0–7.3 (ArH), 7.3–7.6 (ArH), 7.6–7.9 (ArH). IR (thin film), υ (cm^{-1}): 1339 ($-NO_2$). UV–vis (DMF, 0.02 mg/mL): λ_{max} (nm): 480 (nm). IR (thin film), υ (cm^{-1}): 1339 ($-NO_2$).

2.5. General procedure for the synthesis of *P2*–*P4*

P1 (220 mg, 1.00 equiv) was dissolved in DMF (2 mL), then a solution (2 mL) of compound **2** or **3** or **4** (10.0 equiv), 4-(*N*,*N*-dimethyl)aminopyridine (DMAP) (caution: toxic; incompatible with acids and oxidants) (10.0 equiv) and dicyclohexylcarbodiimide (DCC) (caution: moisture sensitive; combustible; incompatible with strong oxidizing agents; avoid exposure to air or moisture) (10.0 equiv) was added. The resultant mixture was stirred at room temperature for 72 h under an atmosphere of dry nitrogen and then filtered to remove the insoluble solid. The filtrate was added dropwise to methanol to precipitate the polymer, which was further purified by several precipitations from THF into methanol, and dried in a vacuum to a constant weight.

P2: red powder (196 mg, 78.2%). $M_w = 8\,570\,000$, $M_w/M_n = 2.08$ (GPC, polystyrene calibration). ^{1}H NMR (DMSO-d6): δ (ppm): 0.4–1.1 ($-CH_3$), 3.4–4.2 ($-NCH_2-$), 4.2–4.7 ($-OCH_2CH_2-$), 6.2–6.8 (ArH), 6.8–7.0 (ArH), 7.0–7.3 (ArH), 7.3–7.6 (ArH), 7.6–7.9 (ArH). IR (thin film), υ (cm^{-1}): 1340 ($-NO_2$). UV–vis (DMF, 0.02 mg/mL): λ_{max} (nm): 480 (nm).

P3: red powder (201 mg, 75.8%). $M_w = 5\,260\,000$, $M_w/M_n = 1.11$ (GPC, polystyrene calibration). ^{1}H NMR (DMSO-d_6): δ (ppm): 0.4–1.1 ($-CH_3$), 3.4–4.2 ($-NCH_2-$), 4.2–4.8 ($-OCH_2CH_2-$), 6.0–6.6 (ArH), 6.8–7.4 (ArH), 7.4–8.2 (ArH), 8.4–8.7 (ArH). IR (thin film), υ(cm^{-1}): 1338 ($-NO_2$). UV–vis (DMF, 0.02 mg/mL): λ_{max} (nm): 480 (nm).

P4: red powder (245 mg, 87.2%). $M_w = 6\,300\,000$, $M_w/M_n = 3.42$ (GPC, polystyrene calibration). ^{1}H NMR (DMSO-d6): δ (ppm): 0.4–1.1 ($-CH_3$), 3.4–4.2 ($-NCH_2-$), 4.2–4.8 ($-OCH_2CH_2-$), 4.8–5.2 ($-CH_2N<$), 6.0–6.6 (ArH), 6.8–7.3 (ArH), 7.3–7.7 (ArH), 7.7–8.0 (ArH). IR (thin film),

υ (cm^{-1}): 1338 (–NO_2). UV–vis (DMF, 0.02 mg/mL): λ_{max} (nm): 480 (nm).

2.6. Synthesis of chromophore **5**

9 (327 mg, 1.65 mmol) were dissolved in an aq solution of 35% hydrochloric acid. The mixture was cooled to 0–5 °C in an ice bath, and then a solution of sodium nitrite (114 mg) in water was added dropwise. After stirred below 5 °C for 15 min, a solution of *N*,*N*-diethylaniline (224 mg, 1.5 mmol) in ethanol was added slowly. The mixture was stirred in the ice bath for another 1 h, some sodium bicarbonate was added to adjust the pH value to 7.0. The reaction mixture was further stirred for 0.5 h, the precipitate was filtered, washed with water. The crude product was purified by column chromatography on silica gel using ethyl acetate/chloroform (1/4) as an eluent to afford red powder (495 mg, 92.1%). ^{1}H NMR ($CDCl_3$) δ (ppm): 1.24 (t, J = 6.6 Hz, 3H, –CH_3), 3.47 (d, J = 6.6 Hz, 4H, –NCH_2–), 3.97 (t, J = 5.4 Hz, 2H, –CH_2OH–), 4.34 (t, J = 4.5 Hz, 2H, –OCH_2–), 6.71 (d, J = 9.3 Hz, 2H, ArH), 7.69 (d, J = 9.6 Hz, 1H, ArH), 7.83 (d, J = 8.7 Hz, 2H, ArH), 7.91 (d, J = 3.9 Hz, 2H, ArH). MS (EI), m/z [M^+]: 358.3 calcd: 358.2.

2.7. General procedure for synthesis of chromophores **6–8**

5 (1.00 equiv), the acid (2, 3 or 4) (2.00 equiv), dicyclohexylcarbodiimide (DCC) (2.00 equiv), 4-(*N*,*N*-dimethyl)aminopyridine (DMAP) (0.20 equiv) were dissolved in dry dichloromethane, then stirred at room temperature for 20 h. the precipitate was filtered, and the crude product was purified by column chromatography.

Chromophore 6. 5 (64 mg, 0.18 mmol), **2** (44 mg, 0.36 mmol). Purified by column chromatography on silica gel using dichloromethane as an eluent to afford red powder (82 mg, 99.0%). IR (thin film), υ (cm^{-1}): 1339 (–NO_2). ^{1}H NMR ($CDCl_3$) δ (ppm): 1.24 (t, J = 7.2 Hz, 6H, –CH_3), 3.46 (d, J = 6.6 Hz, 4H, –NCH_2–), 4.61 (t, J = 4.5 Hz, 2H, –OCH_2–), 4.79 (t, J = 5.1 Hz, 2H, –CH_2CO–), 6.66 (d, J = 7.1 Hz, 2H, ArH), 7.39 (m, 3H, ArH), 7.54 (m, 1H, ArH), 7.71 (d, J = 8.7 Hz, 1H, ArH), 7.84 (d, J = 8.7 Hz, 2H, ArH), 7.89 (d, J = 7.2 Hz, 1H, ArH), 7.98 (s, 1H, ArH), 8.06 (d, J = 7.5 Hz, 1H, ArH). ^{13}C NMR ($CDCl_3$) δ (ppm): 12.9, 45.1, 63.4, 69.1, 111.3, 117.8, 126.8, 128.6, 130.0, 133.3, 144.3, 148.0, 148.1, 151.4, 155.0, 166.7. (EI), m/z [M^+]: 462.4, calcd: 462.2. $C_{25}H_{26}N_4O_5$ (EA) (%, found/calcd): C, 65.06/64.92; H, 5.25/5.67; N, 12.01/12.11.

Chromophore 7. 5 (64 mg, 0.18 mmol), **3** (62 g, 0.36 mmol). Purified by column chromatography on silica gel using dichloromethane as an eluent to afford red powder (90 mg, 98.1%). IR (thin film), υ (cm^{-1}): 1340 (–NO_2). ^{1}H NMR ($CDCl_3$) δ (ppm): 1.21 (t, J = 5.4 Hz, 6H, –CH_3), 3.42 (d, J = 7.2 Hz, 4H, –NCH_2–), 4.66 (t, J = 4.5 Hz, 2H, –OCH_2–), 4.90 (t, J = 4.5 Hz, 2H, –CH_2CO–), 6.57 (d, J = 9.6 Hz, 2H, ArH), 7.44 (m, 2H, ArH), 7.52 (m, 2H, ArH), 7.73 (d, J = 8.7 Hz, 1H, ArH), 7.91 (m, 5H, ArH), 8.22 (d, J = 6.6 Hz, 1H, ArH), 8.94 (d, J = 7.5 Hz, 1H, ArH). ^{13}C NMR ($CDCl_3$) δ (ppm): 12.8, 45.0, 63.3, 68.9, 107.8, 110.9, 111.2, 117.7, 124.8, 126.1, 126.4, 126.8, 128.1, 128.7, 130.8, 131.6, 133.7, 134.0, 144.3, 148.0, 151.3, 155.0, 167.6. (EI), m/z [M^+]: 512.4, calcd: 512.2. $C_{29}H_{28}N_4O_5$ (EA) (%, found/calcd): C, 68.13/67.96; H, 5.71/5.51; N, 10.99/10.93.

Chromophore 8. 5 (64 mg, 0.18 mmol), **4** (81 mg, 0.36 mmol). Purified by column chromatography on silica gel using dichloromethane as an eluent to afford red powder (93 g, 91.9%). IR (thin film), υ (cm^{-1}): 1339 (–NO_2). ^{1}H NMR ($CDCl_3$) δ (ppm): 1.24 (t, J = 5.1 Hz, 6H, –CH_3), 3.47 (d, J = 6.6 Hz, 4H, –NCH_2–), 4.38 (t, J = 4.5 Hz, 2H, –OCH_2–), 4.65 (t, J = 5.1 Hz, 2H, –CH_2CO–), 5.04 (s, 2H, –CH_2N<), 6.68 (d, J = 6.6 Hz, 2H, ArH), 7.30 (m, 7H, ArH), 7.75 (d, J = 2.4 Hz, 1H, ArH), 7.87 (m, 4H, ArH), 8.04 (d, J = 8.1 Hz, 1H, ArH). ^{13}C NMR ($CDCl_3$) δ (ppm): 12.8, 29.9, 44.9, 45.1, 63.6, 68.5, 108.5, 110.6, 111.3, 117.7, 120.0, 120.6, 123.4, 126.1, 126.8, 140.7, 144.3, 147.8, 147.9, 151.5, 154.7, 168.6. (EI), m/z [M^+]: 565.4, calcd: 565.2. $C_{32}H_{31}N_5O_5$ (EA) (%, found/calcd): C, 68.31/67.95; H, 5.98/5.52; N, 12.41/12.38.

2.8. Preparation of polymer thin films

The polymers were dissolved in THF (concentration ~3 wt%) and the solutions were filtered through syringe filters. Polymer films were spin-coated onto indium-tin-oxide (ITO)-coated glass substrates, which were cleaned by DMF, acetone, distilled water and THF sequentially in ultrasonic bath before use. Residual solvent was removed by heating the films in a vacuum oven at 40 °C.

2.9. NLO measurement of poled films

The second-order optical nonlinearity of the polymers was determined by in-situ second harmonic generation (SHG) experiment using a closed temperature-controlled oven with optical windows and three needle electrodes. The films were kept at 45° to the incident beam and poled inside the oven, and the SHG intensity was monitored simultaneously. Poling conditions were as follows: temperature: different for each polymer (Table 1); voltage: 7.0 kV at the needle point; gap distance: 0.8 cm. The SHG measurements were carried out with a Nd:YAG laser operating at a 10 Hz repetition rate and an 8 ns pulse width at 1064 nm. A Y-cut quartz crystal served as the reference.

3. Results and discussion

3.1. Synthesis

The synthetic route to polyphosphazenes was shown in Scheme 1. 2-(2-Hydroxyethoxy)-4-nitrobenzenediazonium fluoroborate was prepared by the similar method as reported previously [50].

Table 1
Polymerization results and characterization data.

no.	Yield (%)	M_w[a]	M_w/M_n[a]	λ_{max}[b] (nm)	λ_{max}[c] (nm)	T_g[d] (°C)	T_d[e] (°C)	T[f] (°C)	l_s[g] (μm)	d_{33}[h] (pm/V)	$d_{33(\infty)}$[i] (pm/V)
P2	78.2	8 570 000	2.08	471 (495)	480 (506)	63	250	56.7	0.46	33.2	4.92
P3	75.8	5 260 000	1.11	472 (496)	480 (508)	70	242	68.2	0.38	40.6	6.03
P4	87.2	6 300 000	3.42	472 (496)	480 (508)	91	261	99.5	0.32	67.3	9.97

[a] Determined by GPC in THF on the basis of a polystyrene calibration.

[b] The maximum absorption wavelength of polymer solutions in THF, while the maximum absorption wavelength of the corresponding small chromophore molecules in diluted THF solutions are given in the parentheses.

[c] The maximum absorption wavelength of polymer solutions in DMF, while the maximum absorption wavelength of the corresponding small chromophore molecules in diluted DMF solutions are given in the parentheses.

[d] Glass transition temperature (T_g) of polymers detected by the DSC analyses under nitrogen at a heating rate of 10 °C/min.

[e] the 5% weight loss temperature of polymers detected by the TGA analyses under argon at a heating rate of 20 °C/min.

[f] the best poling temperature.

[g] film thickness.

[h] Second harmonic generation (SHG) coefficient.

[i] The nonresonant d_{33} values calculated by using the approximate two-level model.

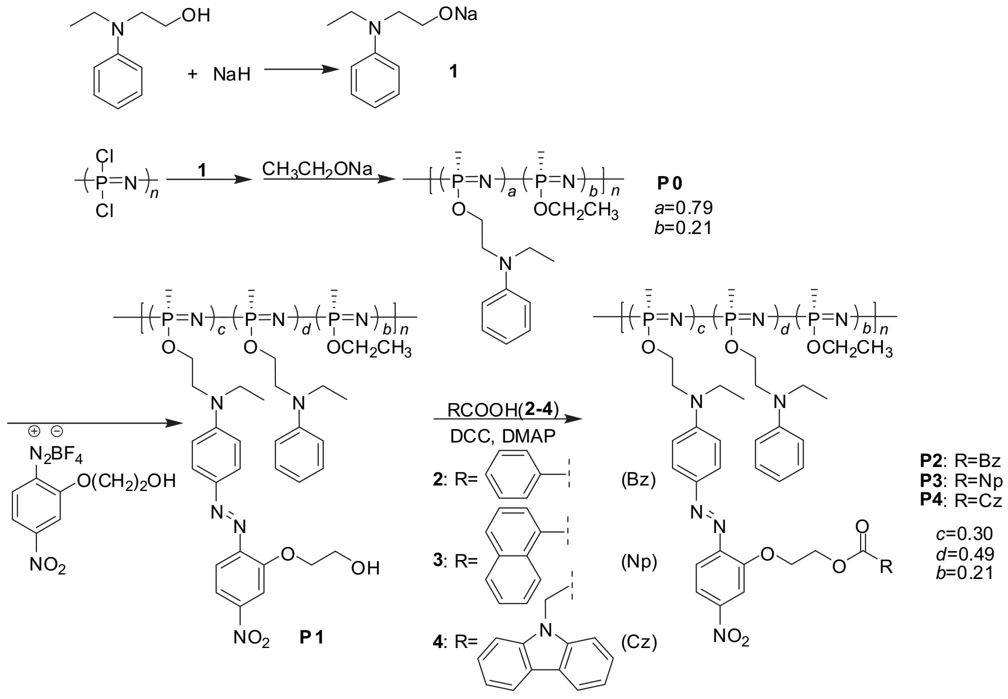

Scheme 1.

Poly(dichlorophosphazene), a highly reactive macromolecular intermediate, was prepared by the thermal ring-opening polymerization of phosphonitrile chloride trimer [1]. **P0** was obtained by nucleophilic substitution reaction from Poly(dichlorophosphazene). As the aniline group could not react with all the chlorine atoms because of the steric shielding effect [51], an excess of $NaOCH_2CH_3$ was added into the reaction mixture to replace all the remaining chlorine atoms completely at the end of the substitution reaction.

Through post-azo coupling reaction, the azobenzene structure in the side chain of polyphosphazene **P1** was constructed efficiently. Different from our previous work, a reactive group-hydroxyl was introduced into the side chain of polyphosphazene for the further functionalization of the chromophore moieties, which could be utilized in the following esterification between **P1** and different carboxylic acids, including benzoic acid (Bz), 1-naphthoic acid (Np) and *N*-carbazolylacetic acid (Cz). These acids were selected as the isolation moieties with different bulk sizes to modify the azobenzene side chains of **P1**. The two-step post-functional polymer reactions, post-azo coupling and esterification reaction, underwent smoothly under very mild conditions while the purification procedure was simple, which was another proof that the post-functional strategy could be an efficient method to modify the polymer structure.

It should be pointed out that the loading density of the chromophore moieties in these polyphosphazenes was really high. As mentioned in the introduction part, in 1991, DR-1 was first linked to the phosphorus–nitrogen backbone for the synthesis of new nonlinear optical (NLO) polymeric materials, and the loading of DR-1 was 33% [25]. As the loading of DR-1 was relatively low, the synthetic procedure was not easy by a direct reaction, Allcock et al. improved their synthetic methods to raise the loading up to 46% via reactions that involved functionalized poly(organophosphazene)s. However, soluble polyphosphazenes with higher percentages of DR-1 moieties could not be obtained by this method. They ascribed these results to the intrinsically high polarity of the donor–acceptor structure of DR-1, the low solubility of the sodium salt of the DR-1 alcohol, and the close packing or stacking of rigid aromatic side groups [25,29]. In 2003, we developed a convenient approach to a polyphosphazene with a high loading density of DR-1 moieties, demonstrating the power and flexibility of the postfunctionalization strategy [31]. Here, through the combination of two post-functional reactions, post-azo coupling and post esterification reactions, soluble polyphosphazenes **P2–4** were conveniently obtained, which bear high loading density of chromophore moieties in the side chains. This further confirmed that the post-functional strategy could be an alternative approach to functional polymers, in

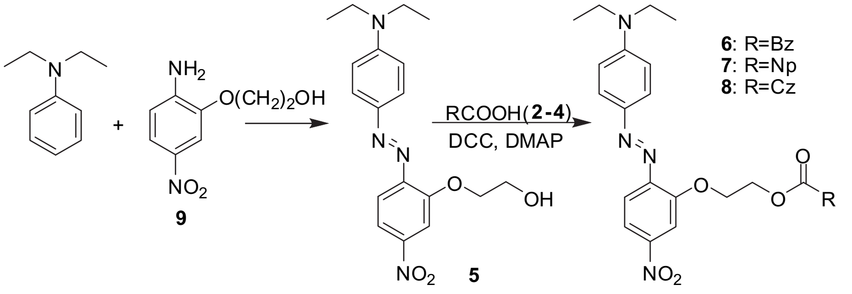

Scheme 2.

addition to the normal synthetic route of the polymerization of the corresponding monomers.

Also, we prepared three model compounds having the similar structure with those attached to the polyphosphazene backbone (Scheme 2). Thus, a comparative study on some properties could be performed between the model compounds and polymers.

3.2. Structural characterization

In the IR spectra of **P0–4** (Fig. 1), the 1250–1200 cm^{-1} bands were attributed to an intense P═N stretching vibration and the 750 cm^{-1} band to an in-phase P-N-P stretch. In comparison with **P0**, **P1–4** showed a new strong absorption band at 1338 cm^{-1}, which should be ascribed to the absorption of nitro groups, confirming the successful introduction of nitro groups into the side chain of polyphosphazenes through the post-azo coupling reaction.

As for all the polymers, the chemical shifts in corresponding ^{1}H NMR spectra verified the proposed structure demonstrated in Scheme 1. The molar concentration of chromophore moieties in **P1** could be calculated by analyzing the ^{1}H NMR peak integration. And its UV–vis spectra gave the similar result. The new absorption peak in the range of 7.3–7.9 ppm should be ascribed to the nitrobenzene moieties. The absorption peak at 4.8–5.0 ppm might be assigned to the hydroxyl group due to its disappearance during heavy water exchange. After the esterification reaction, the absorption peak of the ethylene groups between two oxygen atoms had a downfield shift. For example, in **P3** (Fig. 2), the absorption peak at 3.67 ppm shifted to 4.47 ppm and the peak of the hydroxyl group disappeared, indicating that the hydroxyl group reacted with the added acid completely. Compared with **P0**, the new absorption peaks in **P2–4** at 4.0–5.0 ppm and downfield should be ascribed to the nitrobenzene moieties, which were consistent with ^{1}H NMR spectra of chromophore **6–8** (Figs. 3 and 4).

Polymers **P2–4** were soluble in common polar organic solvents such as THF, DMF, and DMSO, much better than **P1**, which could hardly dissolve in THF. This should be ascribed to the introduction of the isolation groups, as previous cases and confirming the important role the bonded isolation group again. Fig. 5 showed UV–vis spectra of **P2–4** in DMF, and the maximum absorption wavelengths for the π–π^* transition of the azo moieties at 480 nm were nearly unchanged for all three polymers, which means that the introduction of isolation groups did not affect the push-pulls structure of the azobenzene chromophore moieties. That is to say, the electronic properties of the chromophore moieties in polyphosphazenes were just the same before and after the attachment of the isolation groups. So for the NLO properties of **P2–4**, the difference should be caused only by the different size of the isolation groups. In comparison with their corresponding model compounds, the maximum absorption wavelengths of **P2–4** were blue shifted, which might be due to the electronic interaction between the polymer backbone and the NLO chromophores in side chains.

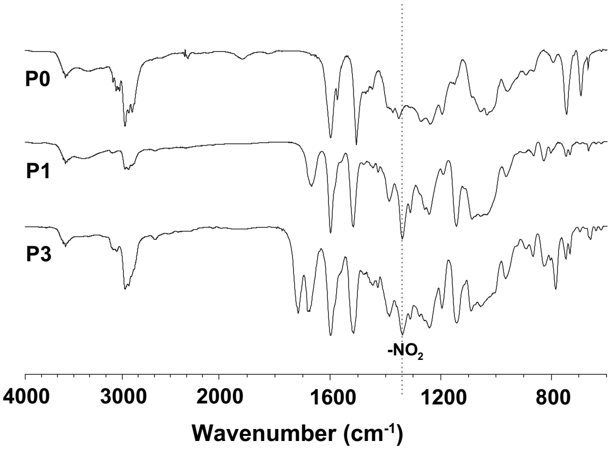

Fig. 1. IR spectra of polymers **P0**, **P1** and **P3**.

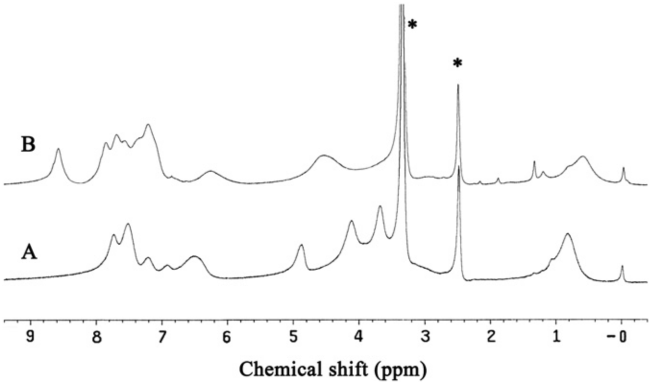

Fig. 2. ^{1}H NMR spectra of **P1** (A) and **P3** (B) in DMSO-*d*6. The solvent peaks are marked with asterisks (*).

The molecular weights of polymers were determined by gel permeation chromatography (GPC) with THF as an eluent and polystyrene standards as calibration standards. All the results were summarized in Table 1, and most of the polymers possessed similar molecular weights, which would perhaps facilitate the comparison of their properties on the same level. Though the molecular weights were high, **P2–4** still showed good solubility in common polar organic solvents such as THF, DMF, and DMSO. The excellent film-forming property of them was beneficial to be spin-coated into thin solid films with proper thickness for the following NLO properties measurement. Their TGA thermograms were shown in Fig. 6, with the 5% weight loss temperatures of polymers listed in Table 1. **P4** exhibited better thermal stability than other polymers, indicating that the introduction of the carbazolyl group to the chromophore would benefit its stability against heating. The glass transition temperatures (T_g) of the polymers were investigated using a differential scanning calorimeter (Table 1). The glass transition temperatures of **P2–4** were low due to the flexible backbone of polyphosphazenes.

3.3. NLO properties

The NLO activity of the polymers were measured similar as we reported previously [37–46,49], which was studied by investigating

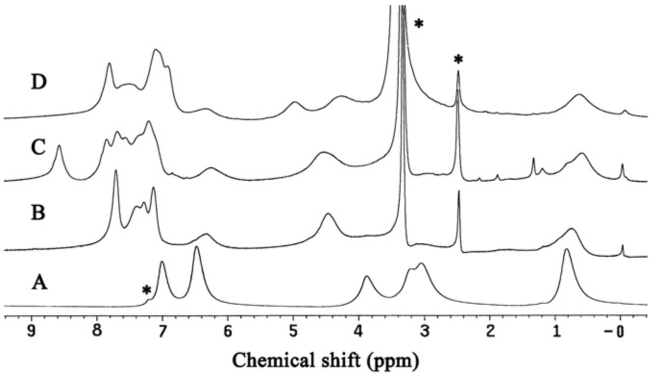

Fig. 3. ^{1}H NMR spectra of **P0** (A) in $CDCl_3$ and **P2–4** (B, C, D) in DMSO-*d*6. The solvent peaks are marked with asterisks (*).

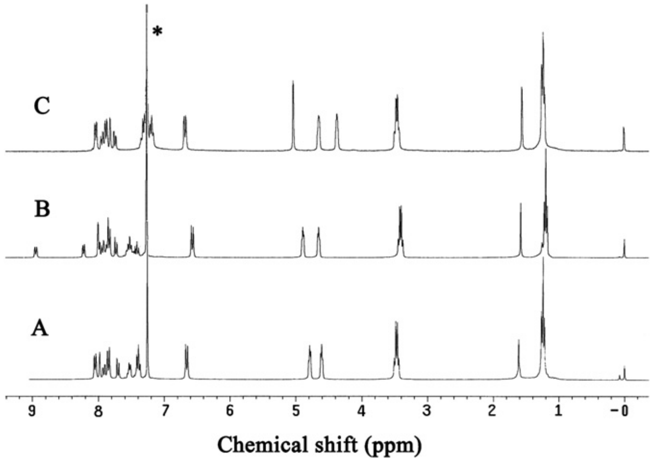

Fig. 4. ^{1}H NMR spectra of **6–8** (A, B, C) in $CDCl_3$. The solvent peaks are marked with asterisks (*).

the second harmonic generation (SHG) processes characterized by d_{33}, an SHG coefficient. And from the experimental data, the d_{33} values of **P2**–**P4** were calculated at the 1064 nm fundamental wavelength (Table 1). The NLO properties of all the polymers were tested at the same time to avoid systematic errors.

To show the NLO results more visually, we compared the d_{33} values of the polymers using that of **P2** as reference in Fig. 7. As expected, the d_{33} values for all of three polymers were much higher than previous ones, which should be benefit from the introduction of isolation groups to interrupt the intermolecular dipole–dipole interactions in some degree. From **P2** to **P4**, the size of isolation group enlarged gradually, while the d_{33} values increased from 33.2 pm/V for **P2** to 67.3 pm/V for **P4**. As discussed above, the similar maximum absorption wavelengths in UV–vis spectra indicated the similar electronic properties of the chromophore moieties in polyphosphazenes. Thus the different NLO properties of the polymers should be caused by difference among the isolation groups, especially related to their size. However, the introduction of different isolation groups would surely lead to the different molar weights of the obtained chromophores. According to the one-dimensional rigid orientation gas model: [52]

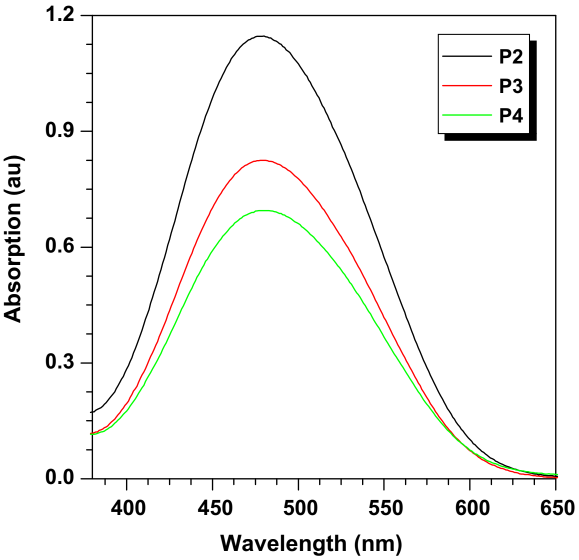

Fig. 5. UV–Vis spectra of DMF solutions of **P2–P4** at the concentration of 0.02 mg/mL.

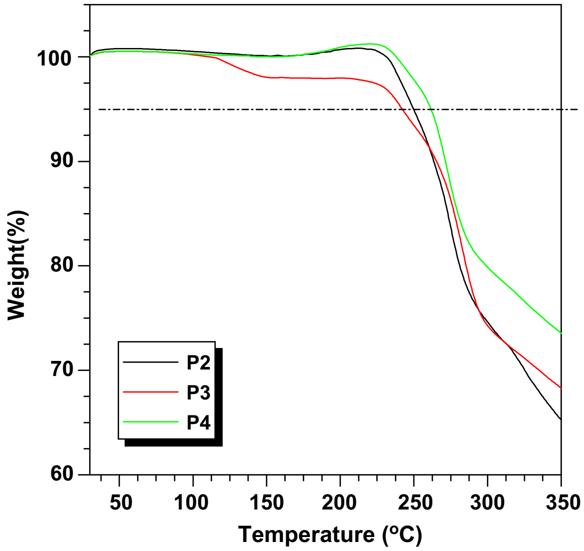

Fig. 6. TGA thermograms of **P2–P4** measured in argon at a heating rate of 10 °C/min.

$$d_{33} = \frac{1}{2} N\beta f^{2\omega} \left(f^{\omega}\right)^2 \left\langle \cos^3\theta \right\rangle \tag{1}$$

where N is the number density of the chromophore, β is its first hyperpolarizability, f is the local field factor, 2ω is the double frequency of the laser, ω is its fundamental frequency, and $<\cos^3\theta>$ is the average orientation factor of the poled film. Here, the active NLO chromophore moieties are the same, which exhibit the same first hyperpolarizability (β), thus under identical experimental conditions, d_{33} should be proportional to the number density of the chromophore moieties in the polymers. Therefore, we considered the different concentrations of the active chromophore moieties in the polymers, using the tested d_{33} values dividing the concentration of the active chromophore moieties in the polymers, and comparing the results again with that of **P2** as references. As a result, the same trend between curve A and curve B could be found, which coincided well with the site isolation principle. Also, we calculated the $d_{33}(\infty)$ values of **P2–4** by using the approximate

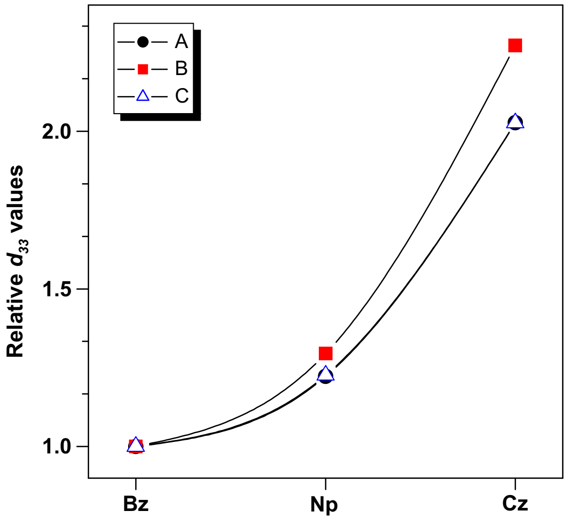

Fig. 7. The analysis of the obtained NLO data of polymers **P2–P4**. A: comparison of the d_{33} values of the polymers; B: comparison of the calculated d_{33} values, which were obtained by using the tested d_{33} values dividing the concentration of the active chromophore moieties of the polymers; C: comparison of the calculated $d_{33(\infty)}$ values according to the approximate two-level model, using **P2** for **P2–P4** as a reference.

two-level model. It was found that the d_{33} (∞) values similarly increased corresponding to the increasing of the size of the isolation group.

Coinciding with the "site isolation principle", in our case, the NLO effect increased with the size of the isolation group. And the carbazolyl moieties should be the most suitable isolation groups for these NLO polyphosphazenes with azobenzene chromophore side chains reported here. Compared with **P2**, the d_{33} value of **P4** with carbazolyl moieties was two times higher. The introduction of isolation groups weakened the strong intermolecular dipole–dipole interactions among the polar chromophore moieties, and benefited to the poling-induced noncentrosymmetric alignment under electric field. Similar as our previous cases, the introduction of carbazolyl moieties as isolation group minimized the electronic interactions greatly, leading to the best NLO property of **P4**.

4. Conclusion

Different isolation groups with different size were introduced to the side chain of NLO polyphosphazenes through the post-functional strategy, by applying the concept of "suitable isolation group". The reaction conditions were mild and the purification procedure was very simple. All the polymers demonstrated good stability, film-forming ability and solubility. Also, we studied the effect of the different size of isolation spacer on the resultant NLO properties. The NLO effects for **P2–4** increased with the size of the isolation groups, with the d_{33} value of **P4** up to 67.3 pm/V. Meanwhile, it was proved that the introduction of an additional reactive group on the side chain, was an efficient strategy to modify the structure of polymers and consequently to optimize their properties.

Acknowledgements

We acknowledge the financial support from the National Natural Science Foundation of China (Project Nos. 20674059).

References

[1] Allcock HR, Kugel RL. Synthesis of high polymeric alkoxy-and aryloxyphosphonitriles. Journal of American Chemical Society 1965;87:4216–7.

[2] Allcock HR. Recent developments in polyphosphazene materials science. Current Opinion in Solid State & Materials Science 2006;10:231–40.

[3] Allcock HR, Steely LB, Kim SH, Kim JH, Kang BK. Plasma surface functionalization of poly[bis(2,2,2-trifluoroethoxy)phosphazene] films and nanofibers. Langmuir 2007;23:8103–7.

[4] Laurencin CT, El-Amin SF, Ibim SE, Willoughby DA, Attawia M, Ambrosio AMA, et al. A highly porous 3-dimensional polyphosphazene polymer matrix for skeletal tissue regeneration. Journal of Biomedical Materials Research 1996;303:133–8.

[5] Nair L, Bhattacharyya S, Bender JD, Greish YE, Brown PW, Allcock H, et al. Fabrication and otimization of methylphenoxy substituted polyphosphazene nanofibers for biomedical applications. Biomacromolecules 2004;5:2212–20.

[6] Allcock HR, Ambrosio AMA. Synthesis and characterization of pH-sensitive poly(organophosphazene) hydrogels. Biomaterials 1996;17:2295–302.

[7] Barrett EW, Phelps MVB, Silva RJ, Gaumond RP, Allcock HR. Patterning poly(organophosphazenes) for selective cell adhesion applications. Biomacromolecules 2005;6:1689–98.

[8] Allcock HR, Phelps MVB, Barrett EW, Pishko MV, Koh W. Ultraviolet photolithigraphic development for polyphosphazene hydrogel microstructures for potential use in microarray biosensors. Chemistry of Materials 2006;18: 609–13.

[9] Tang H, Pintauro PN. Polyphosphazene membranes. IV. Polymer morphology and proton conductivity in sulfonated poly[bis(3-methylphenoxy)phosphazene] films. Journal of Applied Polymer Science 2001;79:49–59.

[10] Lvov SN, Zhou XY, Benning L, Wei XJ, Fedkin MV, Allcock HR, et al. Proceedings of symposium on energy engineering in the 21 Century 2000; p. 1483–8.

[11] Allcock HR, Crane CA, Morrissey CT, Nelson JM, Reeves SD, Honeyman CH, et al. "Living" cationic polymerization of phosphoranimines as an ambient temperature route to polyphosphazenes with controlled molecular weights. Macromolecules 1996;29:7740–7.

[12] Allcock HR, de Denus CR, Prange R, Nelson JM. Synthesis of trifluoromethyl and methyl phosphazene polymers: differences between polymerization and initiator/terminator properties. Macromolecules 1999;32:7999–8004.

[13] Lee M, Katz HE, Erben C, Gill DM, Gopalan P, Heber JD, et al. Broadband modulation of light using an electro-optic polymer. Science 2002;298: 1401–3.

[14] Shi Y, Zhang C, Zhang H, Bechtel JH, Dalton LR, Robinson BH, et al. Low half-wave voltage polymer electro-optic modulators achieved by controlling chromophore shape. Science 2000;288:119–22.

[15] Burland DM, Miller RD, Walsh CA. Second-order nonlinearity in poled-polymer systems. Chemical Reviews 1994;94:31–75.

[16] Ma H, Jen AKY. Functional dendrimers for nonlinear optics. Advanced Materials 2001;13:1201–5.

[17] Moerner WE, Jepsen AG, Thompson CL. Photorefractive polymer. Annual Review of Materials Science 1997;27:585–623.

[18] Barclay GG, Ober CK. Liquid crystalline and rigid-rod networks. Progress in Polymer Science 1993;18:899–945.

[19] Marks TJ, Ratner MA. Design, synthesis, and properties of molecule-based assemblies with large second-order optical nonlinearities. Angewandte Chemie International Edition 1995;34:155–73.

[20] Marder SR, Kippelen B, Jen AKY, Peyghambarian N. Design and synthesis of chromophores and polymers for electro-optic and photorefractive applications. Nature 1997;388:845–51.

[21] Zyss J. Octupolar organic systems in quadratic nonlinear optics: molecules and materials. Nonlinear Optics 1991;1:3–18.

[22] Bai Y, Song N, Gao JP, Sun X, Wang X, Yu G, et al. A new approach to highly electrooptically active materials using cross-linkable, hyperbranched chromophore-containing oligomers as a macromolecular dopant. Journal of American Chemical Society 2005;127:2060–1.

[23] Andreu R, Blesa MJ, Carrasquer L, Garin J, Orduna J, Villacampa B, et al. Two-Photon absorption at telecommunications wavelengths in a dipolar chromophore with a pyrrole auxiliary donor and thiazole auxiliary acceptor. Journal of American Chemical Society 2005;127:7282–3.

[24] Wang Q, Wang LM, Yu LP. Development of fully functionalized photorefractive polymers. Macromolecular Rapid Communications 2000;21:723–45.

[25] Allcock HR, Dembek AA, Kim C, Devine RLS, Shi Y, Steier WH, et al. Second-order nonlinear optical poly(organophosphazenes): synthesis and nonlinear optical characterization. Macromolecules 1991;24:1000–10.

[26] Carriedo GA, Catuxo LF, Alonso FJG, Elipe PG, Gonzalez PA. Preparation of a new type of phosphazene high polymers containing 2,2'-dioxybiphenyl groups. Macromolecules 1996;29:5320–5.

[27] Rojo G, Martin G, Lopez FA, Carriedo GA, Alonso FJG, Martinez JIF. Second-harmonic response and relaxation behavior of high glass-transition temperature polyphosphazene films. Chemistry of Materials 2000;12:3603–10.

[28] Li Z, Qin J, Yang Z, Ye C. Synthesis and nonlinear optical properties of polyphosphazenes with binaphtholyl and indole side groups. Journal of Applied Polymer Science 2007;104:365–71.

[29] Allcock HR, Ravikiran R, Olshavsky MA. Synthesis and characterization of hindered polyphosphazenes via functionalized intermediates: exploratory models for electro-optical materials. Macromolecules 1998;31:5206–14.

[30] Allcock HR, Kim C. Liquid crystalline phosphazenes. High polymeric and cyclic trimeric systems with aromatic azo side groups. Macromolecules 1989;22:2596–602.

[31] Allcock HR, Kim C. Liquid crystalline phosphazenes bearing biphenyl mesogenic groups. Macromolecules 1990;23:3881–7.

[32] Li Z, Qin J, Tang H, Liu Y. Postfunctionalization strategy for developing polyphosphazene with a high loading of highly polar molecules in the side arms. Journal of Applied Polymer Science 2003;89:2989–93.

[33] Fréchet JMJ, Hawker CJ, Gitsov I, Leon JW. Dendrimers and hyperbranched polymers: two families of three-dimensional macromolecules with similar but clearly distinct properties. Journal of Macromolecular Science: Pure and Applied Chemistry 1996;33:1399–425.

[34] Hecht S, Fréchet JMJ. Dendritic encapsulation of function: applying nature's site isolation principle from biomimetics to materials science. Angewandte Chemie International Edition 2001;40:74–91.

[35] Ma H, Chen BQ, Sassa T, Dalton LR, Jen AKY. Highly efficient and thermally stable nonlinear optical dendrimer for electrooptics. Journal of American Chemical Society 2001;123:986–7.

[36] Luo J, Liu S, Haller M, Liu L, Ma H, Alex JKY. Design, synthesis, and properties of highly efficient side-chain dendronized nonlinear optical polymers for electro-Optics. Advanced Materials 2002;14:1763–8.

[37] Li Z, Li Z, Di C, Zhu Z, Li Q, Zeng Q, et al. Structural control of the side-chain chromophores to achieve highly efficient nonlinear optical polyurethanes. Macromolecules 2006;39:6951–61.

[38] Li Z, Zeng Q, Li Z, Dong S, Zhu Z, Li Q, et al. An attempt to modify nonlinear optical effects of polyurethanes by adjusting the structure of the chromophore moieties at the molecular level using "Click" chemistry. Macromolecules 2006;39:8544–6.

[39] Zeng Q, Li Z, Li Z, Ye C, Qin J, Tang BZ. Convenient attachment of highly polar azo chromophore moieties to disubstituted polyacetylene through polymer reactions by using "click" chemistry. Macromolecules 2007;40:5634–7.

[40] Li Z, Li P, Dong S, Zhu Z, Li Q, Zeng Q, et al. Controlling nonlinear optical effects of polyurethanes by adjusting isolation spacers through facile postfunctional polymer reactions. Polymer 2007;47:3650–7.

[41] Li Z, Dong S, Yu G, Li Z, Liu Y, Ye C, et al. Novel second-order nonlinear optical main-chain polyurethanes: adjustable subtle structure, improved thermal stability and enhanced nonlinear optical property. Polymer 2007;47:5520–9.

[42] Li Z, Zeng Q, Yu G, Li Z, Ye C, Liu Y, et al. New azo chromophore-containing conjugated polymers: facile synthesis by using "Click" chemistry and enhanced nonlinear optical properties through the introduction of suitable isolation groups. Macromolecular Rapid Communications 2008;29:136–41.

[43] Li Z, Yu G, Li Z, Liu Y, Ye C, Qin J. New second-order nonlinear optical polymers containing the same isolation groups: optimized syntheses and nonlinear optical properties. Polymer 2008;49:901–14.

[44] Li Q, Li Z, Ye C, Qin J. Nonlinear optical chromophores with pyrrole moieties as the conjugated bridge: enhanced NLO effects and interesting optical behavior. Journal of Physical Chemistry B 2008;112:4928–33.

[45] Li Q, Yu G, Huang J, Liu H, Li Z, Ye C, et al. Polyurethanes containing indole-based non-linear optical chromophores: from linear chromophore to H-Type. Macromolecular Rapid Communications 2008;29:798–803.

[46] Li Q, Li Z, Zeng F, Gong W, Li Z, Zhu Z, et al. From controllable attached isolation moieties to possibly highly efficient nonlinear optical main-chain polyurethanes containing indole-based chromophores. Journal of Physical Chemistry B 2007;111:508–14.

[47] Li Z, Yu G, Dong S, Wu W, Liu Y, Ye C, et al. The role of introduced isolation groups in PVK-based nonlinear optical polymers: enlarged nonlinearity, improved processibility, and enhanced thermal stability. Polymer 2009;50:2806–16.

[48] Li Z, Dong S, Li P, Li Z, Liu Y, Ye C, et al. New PVK-based nonlinear optical polymers: enhanced nonlinearity and improved transparency. Journal of Polymer Science Part A: Polymer Chemistry 2008;46:2983–93.

[49] Zhu Z, Li Q, Zeng Q, Li Z, Li Z, Qin J, et al. New azobenzene-containing polyurethanes: post-functional strategy and second-order nonlinear optical properties. Dyes and Pigments 2008;78:199–206.

[50] Starkey EB, Smith LI, Ungnade HE. *p*-Dinitrobenzened. Organic Syntheses 1943;2:225–7.

[51] Allcock HR. Phosphazene high polymers. In: Allen SG, Bevington JC, editors. Comprehensive polymer science. Oxford: Pergamon Press; 1989. p. 525–32.

[52] Moylan CR, Miller RD, Twieg RJ, Lee VY, McComb IH, Ermer S, et al. Defeating tradeoffs for nonlinear optical chromophores. Proceedings of SPIE 1995;2527:150–62.